OSL-thermochronometry using bedrock quartz

A note of caution

Guralnik, B.; Ankjærgaard, C.; Jain, M.; Murray, A.S.; Müller, A.; Wälle, M.; Lowick, S.E.; Preusser, F.; Rhodes, E.J.; More Authors

DOI
10.1016/j.quageo.2014.09.001

Publication date
2015

Document Version
Final published version

Published in
Quaternary Geochronology

Citation (APA)
Guralnik, B., Ankjærgaard, C., Jain, M., Murray, A. S., Müller, A., Wälle, M., Lowick, S. E., Preusser, F., Rhodes, E. J., & More Authors (2015). OSL-thermochronometry using bedrock quartz: A note of caution. *Quaternary Geochronology*, *25*, 37-48. https://doi.org/10.1016/j.quageo.2014.09.001

Important note
To cite this publication, please use the final published version (if applicable).
Please check the document version above.

Quaternary Geochronology 25 (2015) 37–48

Contents lists available at ScienceDirect

Quaternary Geochronology

journal homepage: www.elsevier.com/locate/quageo

Research paper

OSL-thermochronometry using bedrock quartz: A note of caution

B. Guralnik [a, b, *], C. Ankjærgaard [c, d], M. Jain [b], A.S. Murray [e], A. Müller [f, g], M. Wälle [a], S.E. Lowick [h], F. Preusser [i], E.J. Rhodes [j], T.-S. Wu [k], G. Mathew [l], F. Herman [m]

[a] Department of Earth Sciences, ETH, 8092 Zurich, Switzerland
[b] Center for Nuclear Technologies, Technical University of Denmark, DTU – Risø Campus, Roskilde, Denmark
[c] Netherlands Centre for Luminescence Dating, Soil Geography and Landscape Group, Wageningen University, Wageningen, The Netherlands
[d] Faculty of Applied Sciences, Delft University of Technology, Mekelweg 15, 2629JB Delft, The Netherlands
[e] Nordic Laboratory for Luminescence Dating, Department of Geoscience, Aarhus University, DTU Risø Campus, Denmark
[f] Geological Survey of Norway, POB 6315 Sluppen, 7491 Trondheim, Norway
[g] Natural History Museum of London, Cromwell Road, London SW7 5BD, UK
[h] Institute of Geological Sciences, University of Bern, Baltzerstrasse 1+3, 3012 Bern, Switzerland
[i] Department of Physical Geography and Quaternary Geology, Stockholm University, 10691 Stockholm, Sweden
[j] Department of Earth, Planetary, and Space Sciences, UCLA, Los Angeles, CA 90095-1567, USA
[k] Department of Geosciences, National Taiwan University, No. 1, Sec. 4, Roosevelt Road, Taipei 10617, Taiwan
[l] Department of Earth Sciences, Indian Institute of Technology, Bombay, Powai 400 076, India
[m] Institute of Earth Surface Dynamics, University of Lausanne, Geopolis 3232, 1015 Lausanne, Switzerland

ARTICLE INFO

Article history:
Received 28 February 2014
Received in revised form
6 September 2014
Accepted 10 September 2014
Available online 16 September 2014

Keywords:
OSL-thermochronometry
TR-OSL
Quartz
Fast OSL component
LA-ICP-MS

ABSTRACT

Optically stimulated luminescence (OSL) thermochronometry is an emerging application, whose capability to record sub-Million-year thermal histories is of increasing interest to a growing number of subdisciplines of Quaternary research. However, several recent studies have encountered difficulties both in extraction of OSL signals from bedrock quartz, and in their thermochronometric interpretation, thus highlighting the need for a methodological benchmark. Here, we investigate the characteristic OSL signals from quartz samples across all major types of bedrock and covering a wide range of chemical purities. High ratios of infrared to blue stimulated luminescence (IRSL/BLSL), an insensitive 'fast' OSL component, and anomalously short recombination lifetimes seen in time-resolved luminescence (TR-OSL), are often encountered in quartz from crystalline (magmatic and metamorphic) bedrock, and may hamper successful OSL dating. Furthermore, even when the desirable signal is present, its concentration might be indistinguishable from its environmental steady-state prediction, thus preventing its conversion to a cooling or heating history. We explore the saturation properties and the thermal activation parameters of various OSL signals in quartz to outline the capabilities and limitations for their use in low-temperature thermochronometry.

1. Introduction

Although the potential of luminescence to reconstruct thermal histories of rocks (thermochronology) has been recognized since the early 1950's (Daniels et al., 1953), luminescence thermochronometry has received only a sporadic interest outside of the archaeological research (dating fired pottery and heated stones; see Wintle, 2008). A few notable exceptions include (i) a reconstruction of the atmospheric entry temperatures of terrestrial meteorites (Houtermans et al., 1957), (ii) the dating of volcanic dike emplacement (Johnson, 1963), (iii) determination of the ambient temperatures on the surface of Earth (Ronca and Zeller, 1965) and Moon (Durrani et al., 1977), and (iv) the characterisation of a volcanic geothermal field (Tsuchiya et al., 2000). Recently, an increasing interest in luminescence-based thermochronology has been re-ignited by Herman et al. (2010). These authors measured optically stimulated luminescence (OSL) ages of bedrock quartz in New Zealand, interpreting the obtained data as 'cooling ages' which confirmed the Quaternary erosion rate of the Southern Alps on a previously unaddressed timescale (~0.1 Ma).

In the years following the introduction of OSL-thermochronometry (Herman et al., 2010), major concerns have been raised both in regard to the suitability of standard OSL dating

* Corresponding author. Department of Earth Sciences, ETH, 8092 Zurich, Switzerland.
E-mail address: benny.guralnik@gmail.com (B. Guralnik).

http://dx.doi.org/10.1016/j.quageo.2014.09.001
1871-1014/

protocols to bedrock quartz (Sohbati et al., 2011), and to the validity of relating such luminescence dates to apparent closure temperatures (Li and Li, 2012). While the latter issue has been recently resolved through a revised closure theory (Guralnik et al., 2013), the purely methodological question, i.e. the suitability of bedrock quartz for reliable OSL dating, still stands open. As highlighted by De Sarkar et al. (2013), the problem with bedrock quartz mechanically separated from a crushed crystalline rock is that it often contains a rather unfavourable combination of dim and slow OSL components (e.g. Preusser et al., 2009) further overprinted by luminescence from feldspar inclusions or fragments (e.g. Short and Huntley, 1992; Huntley et al., 1993). Given that feldspar contamination in quartz typically requires signal removal and/or filtering (Rendell and Wood, 1994; Thomsen et al., 2008a; Ankjærgaard et al., 2010b), while slow OSL components are often considered unreliable for dating (Singarayer, 2003; Preusser et al., 2009), a combination of the two is even more challenging in regard to extracting a useful signal for dating. However, neither of these problems have been sufficiently presented and/or discussed in previous OSL-thermochronometry studies.

Here we re-evaluate the luminescence signal quality of bedrock quartz from all previous OSL-thermochronometry and related studies (Herman et al., 2010; Wu et al., 2012; Dehnert et al., 2012; De Sarkar et al., 2013) against standard OSL characteristics of reference luminescence materials (Murray et al., 1997; Buylaert et al., 2011) and of a suite of naturally-occurring high-purity quartz (HPQ). We then explore the limitations of OSL-thermochronometry regardless of the signal quality, but arising from characteristic saturation (Li and Li, 2012; Guralnik et al., 2013). Numerical analysis highlights the geological scenarios under which various OSL components can be expected to be found in either saturation, or thermal steady-state, thus preventing reliable dating and/or extraction of useful paleothermal information.

2. Diagnostic tools for assessing quartz luminescence and chemistry

2.1. Optical cross section

Continuous-wave (CW) optical stimulation of quartz can be described as a sum of first-order decays from distinct electron traps, each with a characteristic photo-ionization cross-section σ_i [cm^2] (Bailey et al., 1997). The decay lifetime τ_i [s] of a certain trap (or component) is further related to the specific power density P of the stimulating source [W cm^{-2}], and the stimulation wavelength λ [cm], through $\tau_i = hc/\lambda P\sigma_i$, where h is Planck's constant and c is the speed of light (Choi et al., 2006). This relationship allows normalisation of a luminescence decay curve to any particular experimental setup, thus enabling a global comparison of quartz samples in terms of their optical cross-sections (Durcan and Duller, 2011). In this work, we evaluate the sample-specific optical cross sections against the well-constrained value of $(2.60 \pm 0.06) \times 10^{-17}$ cm^2 (Durcan and Duller, 2011), which corresponds to the 'fast component' used in standard OSL geochronology (Wintle and Murray, 2006 and references therein).

2.2. IRSL/BLSL ratio

Despite the ambiguity regarding whether pure quartz can (Godfrey-Smith and Cada, 1996; Poolton et al., 1997) or cannot (Baril, 2004) be optically stimulated with infrared light, the relative magnitudes of the infrared stimulated luminescence (IRSL) and the blue-light stimulated luminescence (BLSL) do serve as a good relative diagnostic of quartz purity (Smith et al., 1990; Duller, 2003). Here, we adopt a heuristic test, devised by Vanderberghe et al. (2003) and later formalized by Buylaert et al. (2008), known as the 'IRSL/BLSL ratio'. Representing a quick and costless alternative to the more extended 'OSL-IR depletion' test (Duller, 2003), the IRSL/BLSL ratio is obtained by dividing the light sums of the IRSL and the subsequently measured BLSL signals from the initial 0.8 s of each optical stimulation (following the same irradiation dose). Since IRSL/BLSL ratios exceeding 10% have been related to systematic underestimation of equivalent doses (Buylaert et al., 2008), we follow these authors in regarding such signals as contaminated, and thus undesirable for dating.

2.3. Recombination centre lifetimes

Optical stimulation of quartz using pulsed light (with pulse duration on the microsecond scale; Sanderson and Clark, 1994; Bøtter-Jensen et al., 2003) allows the determination of the relaxation lifetimes of the participating recombination centres (Chithambo and Galloway, 2000a; Lapp et al., 2009). The relaxation lifetime of the main recombination centre in quartz has been extensively studied (Chithambo and Galloway, 2000a,b; Bailiff, 2000; Pagonis et al., 2014a and references therein). In this work, we adopt an average value of 37 ± 3 μs (Ankjærgaard et al., 2010b; constrained on 30 samples), which provides a representative diagnostic of the typical luminescence behaviour of quartz used in standard OSL geochronology.

2.4. Chemistry

Although quartz is one of the purest minerals on Earth, it often contains solid micro-inclusions of zircon, apatite, monazite, feldspar, mica, etc., usually with dimensions of 50 μm or less (e.g. Götze, 2012). Here, we determine the chemical purity of the obtained quartz samples using laser-ablation inductively coupled plasma mass spectrometry (LA-ICP-MS), and evaluate the results against the high-purity quartz (HPQ) baseline of Müller et al. (2012), which stringently limits the foreign element concentrations in quartz to Al < 30, Ti < 10, Na < 8, K < 8, Ca < 5, Li < 5, Fe < 3, P < 2 and B < 1 (all values in μg g^{-1}).

3. Materials and methods

3.1. Samples

The ten samples used in this study (nine quartzes and one feldspar) are fully listed in Table 1. The quartz samples encompass all bedrock types (3 sedimentary, 5 metamorphic, and 1 magmatic), and are further ordered by their metamorphic grade. The above dataset includes all previously published OSL-thermochronometry samples (K0587, METASS01, TWNG6 and KTB218A), a related study (NWE1), three high-purity natural quartzes (GA2, DRAG and GULL) each with an exceptionally low amount of trace elements (<50 μg g^{-1} in total), and a sedimentary quartz with which the single aliquot regenerative-dose (SAR) protocol was developed (WIDG8). The concluding feldspar sample (FK981014) has been subjected to an identical analysis, to allow its possible identification as a luminescence contaminant in the quartz signals.

3.2. Instrumentation

Luminescence characterisation of the four previously reported materials (K0587, METASS01, NWE1 and TWNG6) is documented in their respective papers (see Table 1). A more extensive analysis of the other six samples (GA2, DRAG, GULL, WIDG8, KTB218A and FK981014) was undertaken using an automated Risø TL/OSL reader DA-20 (Bøtter-Jensen, 1997), with an inbuilt $^{90}Sr/^{90}Y$ beta source

Table 1
Mineral samples used in this study.

Sample	Rock sample	Metamorphic grade	Relevant studies	Aliquot description
WIDG8	Unconsolidated sand (Widgingarri, Australia)	None (O'Connor, 1999; Murray et al., 1997)	SAR protocol development (Wintle and Murray, 2006 and references therein), and various luminescence characteristics (Wintle and Murray, 1997; Murray et al., 1997; Murray and Wintle, 1999; Choi et al., 2006; Ankjærgaard et al., 2008, 2010a; Pagonis et al., 2010; Durcan and Duller, 2011)	Separated and etched quartz (90–125 μm) with identified inclusions of zircon, feldspar, and apatite
NWE1	Weakly consolidated sandstone (Niederweningen, Switzerland)	Shallow diagenesis, <60 °C, <0.5 kbar (Monnier, 1982)	Luminescence properties (Dehnert et al., 2012)	Separated and etched quartz (4–11 μm)
META-SS01	Meta-sandstone (Central range, Taiwan)	Prehnite-pumpellyite to greenschist, 330–375 °C, 3–4 kbar (Beyssac et al., 2007; Kidder et al., 2013)	Assessment for utilization in OSL-thermochronology (Wu et al., 2012)	Separated and etched quartz (90–150 μm) from hand-crushed rock groundmass
K0587	Chlorite-greenschist (Whataroa basin, New-Zealand)	Greenschist >400 °C, >5 kbar (Grapes and Watanabe, 1992)	OSL-thermochronology (Herman et al., 2010)	Separated and etched quartz (90–210 μm) from hand-crushed rock groundmass
GULL	Kyanite quartzite (Gullsteinberget, Norway)	Upper greenschist to amphibolite, >420 °C, >2.8 kbar (Müller et al., 2012)	Quartz chemistry (Müller and Koch-Müller, 2009; Müller et al., 2007; Müller et al. 2012)	Polycrystalline high purity quartz (HPQ), hand-crushed to 100–200 μm, with identified inclusions of pyrophyllite, muscovite, rutile, pyrite and zircon, and devoid of feldspar inclusions.
DRAG	Pegmatitic quartz vein (Nedre Øyvollen, Norway)	Amphibolite 420–450 °C, 2–3 kbar (Müller et al., 2012)	Quartz chemistry (Götze et al., 2004; Müller et al., 2012)	Polycrystalline HPQ (hand-crushed to 100–200 μm) with identified fluid inclusions, and extremely rare microinclusions of albite and biotite; hand-crushed to 100–200 μm
GA2	Hydrothermal quartz vein (Gamsberg, Namibia)	Amphibolite 630–670 °C, 2.8–4.5 kbar (Stalder and Rozendaal, 2004)	Quartz chemistry (Kronz et al., 2012)	Monocrystalline HPQ (hand-crushed to 100–200 μm) with identified rare fluid and CO_2 inclusions.
TWNG6	Garnet–sillimanite-gneiss (Western Arunachal Himalaya, India)	Upper amphibolite 535–715 °C, 7–9 kbar (Warren et al., 2014)	OSL-thermochronology (De Sarkar et al., 2013)	Separated and etched quartz (90–150 μm) from hand-crushed rock groundmass
KTB-218A	Garnet-sillimanite-biotite-gneiss (Windisch-eschenbach, Germany)	Upper amphibolite 680–720 °C, 8–9 kbar (Reinhardt, 1997)	Gneiss chemistry (Reinhardt, 1997), thermochronology (Wagner et al., 1997; references therein; Wolfe and Stockli, 2010), and luminescence characteristics of extracted quartz (Prokein and Wagner, 1994).	Separated and etched quartz (180–212 μm) from hand-crushed rock groundmass (borehole depth of 914 m), with identified inclusions of plagioclase, zircon, monazite, apatite, kyanite, and muscovite.
FK- 981014	Fossilferous sandstone and claystone (Gammelmark, Denmark)	Shallow diagenesis (Buylaert et al., 2011)	Luminescence characteristics (Murray et al., 2009; Buylaert et al., 2009, 2011, 2012a; Thomsen et al., 2011)	Sieved and etched feldspar (90–150 μm)

delivering a calibrated dose rate of ~0.2 Gy s^{-1}. Stimulation involved two different optical sources: (i) infrared (870 ± 40 nm) light-emitting diode (LED) array, delivering a total of ~135 mW cm^{-2} at the sample position, and (ii) blue light (470 ± 30 nm) LED array, delivering a total of ~45 mW cm^{-2} at the sample position (Bøtter-Jensen, 1997). All luminescence was stimulated using an integrated pulsing option on the DA-20 reader to control the blue and infrared LEDs, and was detected using a photomultiplier tube (EMI QA 9235) and a photon timer attachment (based on an ORTEC 9353 100 ps time digitizer board) as described in Lapp et al. (2009). The duration of each stimulation pulse (on-time) and of the pause in-between stimulations (off-time) was 50 μs and 200 μs, respectively. Detection of IRSL was done through a combination of a 2 mm Schott BG39 and a 4 mm Corning 7–59 filters, while BLSL was detected using a 7.5 mm Schott U-340 glass filter (Bøtter-Jensen, 1997). IRSL and BLSL were sequentially measured following a standard preheat to 260 °C for 10 s. To minimise any possible effects of thermal assistance and to make the IRSL and BLSL data directly comparable, all optical stimulations were conducted at 60 °C. Thermal annealing of the samples GA2, DRAG, GULL, and KTB218A was carried out at 650 °C for 10 min.

Concentrations of Al, Ti, Na, K, Ca, Fe, Li, B, and P in six samples (GA2, DRAG, GULL, WIDG8, KTB218A and FK981014) were measured by laser-ablation inductively coupled plasma mass spectrometry (LA-ICP-MS), using the facilities at the Geological Survey of Norway (New-Wave 193 nm excimer laser coupled to a Thermo Element 1 ICP-MS), and at the Department of Earth Sciences of ETH-Zürich (GeoLas 193 nm ArF excimer laser connected to a Perkin Elmer Elan 6100 DRC). The lasers had spot sizes of 10–60 μm, and repetition rates of 10–20 Hz. Raster ablation was typically applied in the centre of each quartz crystal or grain, with an approximate depth of ablation of 20–50 μm. The analytical errors ranged within 10% of the absolute concentration of each element (Müller et al., 2012, and references therein). Furthermore, the concentration variance across each crystal (due to chemical inhomogeneity) was ~30% (on average) for the HPQ suite, and ~70% (on average) for the standard purity quartzes (WIDG8 and KTB218A) and feldspar (FK981014).

3.3. Data analysis

Recognition of various luminescence components in quartz was performed using a multiexponential analysis. As a rule, luminescence decay curves (both CW-OSL and TR-OSL) in quartz may be represented by a sum of exponentially-decaying components $I(t) = \sum_i I_i \exp(-t/\tau_i)$, where τ_i is the characteristic decay lifetime

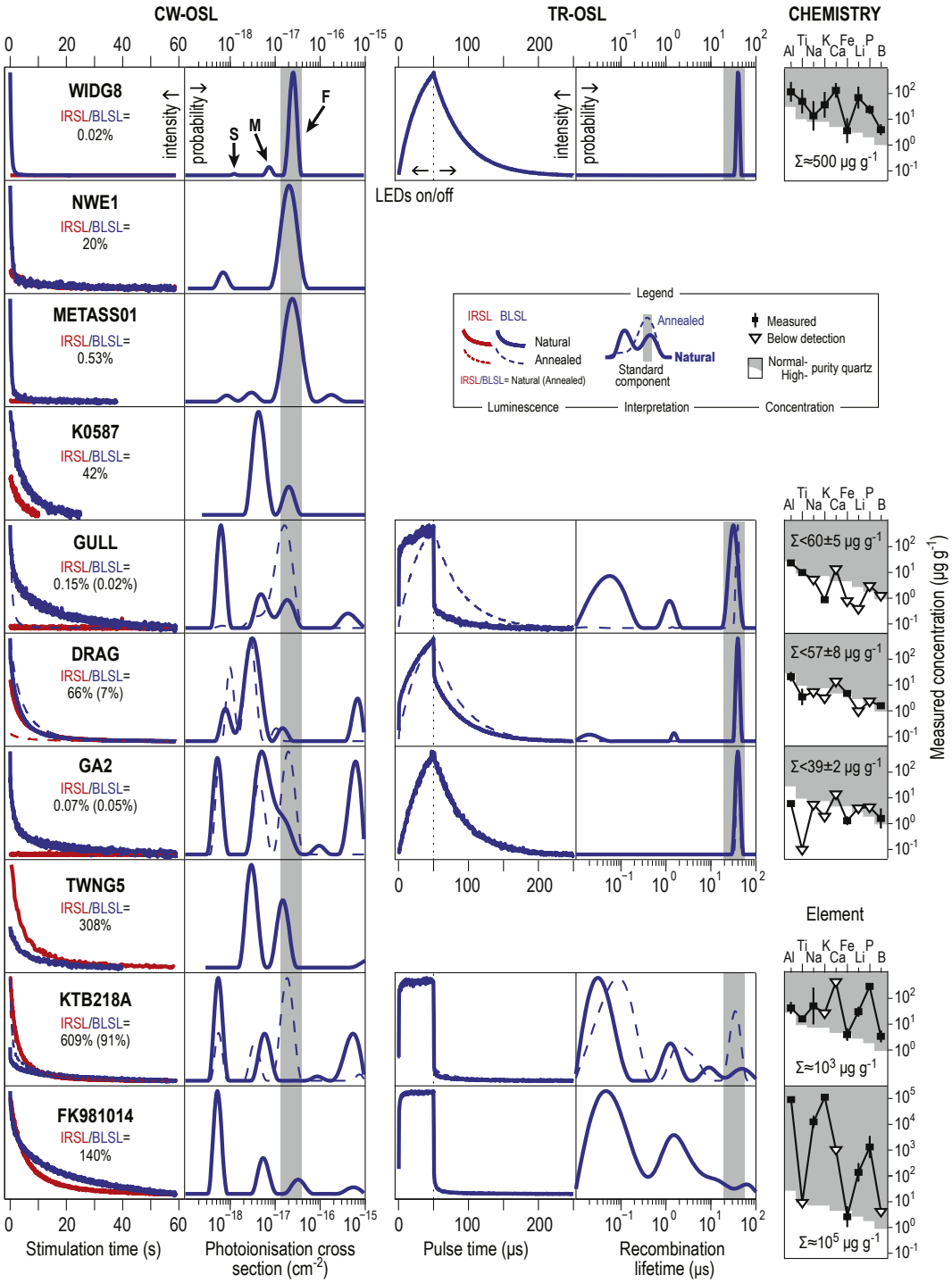

Fig. 1. CW-OSL (columns 1–2), TR-OSL (columns 3–4), and geochemical (column 5) results for quartz samples sorted based on their metamorphic grade, and concluded with a reference feldspar (see Table 1). Columns 2 and 4 display the multi-exponential deconvolution of data in columns 1 and 3 (respectively), with grey bands highlighting the desired components (see text). The power density of the blue LEDs was 15 mW cm^{-2} for TWNG5, 18 mW cm^{-2} for K0587, 37 mW cm^{-2} for NWE1, and 45 mW cm^{-2} elsewhere.

of the i-th component, I_i and $I(t)$ are its initial and instantaneous luminescence intensity [a.u.], and t the time. The underlying components of any arbitrary $I(t)$ may be found using a linearized solution of the Fredholm integral equation of the first kind, which assumes a continuous distribution of decay lifetimes, and obtains their corresponding amplitudes via linear inversion (Whittall and MacKay, 1989; Singarayer, 2003; Ankjærgaard et al., 2010a). Here, we use MERA, a Multi-Exponential Relaxation Analysis Toolbox for Matlab (Horch et al., 2011, 2012), which is freely available at http://vuiis.vanderbilt.edu/~doesmd/MERA/MERA_Toolbox.html, and allows the visualisation of the inverted amplitudes as a normalized probability density function.

To evaluate the thermochronometric usability of a certain luminescence signal of interest (Guralnik et al., 2013), we consider the characteristic rate equation $dn/dt = (\dot{D}/D_0)(N-n) - ns\exp(-E/k_BT)$, in which E [eV] and s

[s^{-1}] are the thermal activation (Arrhenius) parameters of the electron trap, n is the instantaneous number of trapped electrons in N available traps, $\dot{D}$ [Gy s^{-1}] and D_0 [Gy] the natural dose rate and the characteristic dose, T [K] the temperature, and k_B Boltzman's constant (Christodoulides et al., 1971). More specifically, we couple this rate equation to a simple thermal scenario dT/dt = const, where const is a linear heating or cooling rate [°C Ma^{-1}]. The simulations involve solving the coupled differential equations for arbitrary heating or cooling rates, and yield the fractional trap filling n/N as a function of the instantaneous temperature. To distinguish between signals associated with transient thermal processes versus signals reflecting ambient thermal conditions, we compare the simulated n/N values to their corresponding environmental steady-state concentrations, given by $(n/N)_{SS} = [s\exp(-E/k_BT) \times D_0/\dot{D} + 1]^{-1}$ (Eq. A.9b in Guralnik et al., 2013).

4. Luminescence characteristics of bedrock quartz

4.1. Variability of BLSL components with metamorphic grade

The obtained luminescence and chemical data for the nine studied quartz samples are presented in Fig. 1, where they are ordered according to the metamorphic grade of their parent rock; the list is concluded by a feldspar sample, serving as a reference for the most common signal contamination in quartz. The top row of Fig. 1 shows the luminescence characteristics of sample WIDG8, which has been used in the development of the standard OSL dating protocol (Wintle and Murray, 2006 and references therein). The luminescence of this aeolian (unmetamorphosed) sand is characterised by a rapid CW-BLSL decay (solid blue line (in web version) in the first column), reaching near-background intensity within only a few seconds of optical stimulation. Deconvolution of this CW-BLSL signal (second column), reveals the dominance of a single exponential component, known as the 'fast' component ('F' in Fig. 1), and rather negligible contributions from the 'medium' ('M') and 'slow' ('S') components (Bailey et al., 1997). This behaviour is regarded as 'exemplary' due to an excellent correlation between OSL dates obtained using the fast component and independent geochronometers (Murray and Olley, 2002; Rittenour, 2008), and thus serves as a valid baseline for evaluating OSL signals from other quartz samples.

Comparison of the CW-BLSL decay curves (solid blue lines (in web version) in the first column of Fig. 1) reveals that only the low-metamorphic grade samples NWE1 and METASS01 exhibit comparably rapid luminescence decay to WIDG8. The remaining quartzes, originating from higher-grade metamorphic or magmatic rocks, show a profoundly slower CW-BLSL decay, and thus a much smaller contribution from the fast component. To quantify this, we use the well-constrained photoionisation cross section of the fast OSL component ($\sigma_F = 2.60 \pm 0.06 \times 10^{-17}$ cm^2; Durcan and Duller, 2011; see Section 2.1) to evaluate the relative intensity of this component in all samples. The output of our multiexponential fitting is a peak-shaped density distribution of photoionisation cross-section probabilities (second column in Fig. 1), and not a finite number of discrete components with associated errors. To evaluate such peak-shaped data against the rather narrow estimate of σ_F, we assign a larger window for the fast component integration than that given just by the uncertainty on σ_F. More specifically, we set the integration window for the fast component (grey band in column 2, Fig. 1) to between 1.30×10^{-17} cm^2 and 3.90×10^{-17} cm^2, corresponding to 50% error about σ_F, which is comparable to the full width at half maximum (FWHM) of most of the inverted peaks.

Fig. 2 shows the relative intensity of the fast CW-BLSL component plotted against the estimated metamorphic temperature of the corresponding parent rock (column 3 in Table 1). Although the dataset is of very limited size ($n = 9$), it does suggest a pattern: the fast component seems to dominate the natural OSL signal in mature sedimentary quartz (WIDG8) and low-grade (<350 °C) metamorphic metapelites (NWE1 and METASS01), while being only a secondary constituent (<30%) in quartz of magmatic (DRAG) and higher-grade metamorphic (TWNG6, K0587, GULL, GA2 and KTB218A) origin. In fact, the minute (<10%) presence of the 'fast' component in samples GA2, DRAG and KTB218A is comparable to that spuriously detected in feldspar (FK981014) – a mineral with a completely different set of electron traps and recombination centres (Krbetschek et al., 1997), and whose luminescence essentially defies a simple breakdown into first-order components (Pagonis et al., 2014b and references therein). This suggests that very dim (<10%) intensity of the fast OSL component in quartz could in fact all originate from feldspar inclusions or contaminants, and thus should not be used for quartz OSL dating.

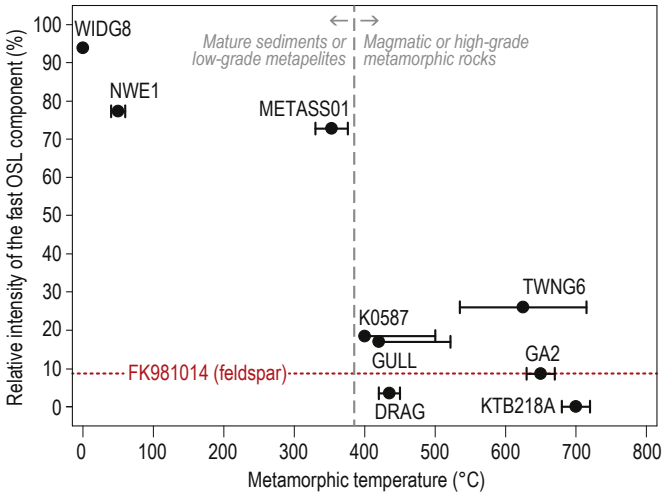

Fig. 2. Relative intensity of the fast OSL component in bedrock quartz as a function of the estimated metamorphic temperature. Horizontal dotted line corresponds to the spurious level of this component as extracted from the reference feldspar, and thus may serve as a detection threshold. Vertical dashed line empirically divides between quartz in which the fast component is dominant (sediments and low-grade metapelites), and those where it is only a minor constituent (high-grade metamorphic and magmatic rocks).

4.2. Variability of BLSL components with chemical purity

The three samples GA2, DRAG and GULL correspond to some of the chemically purest quartz that occurs in nature (Müller et al., 2012; Kronz et al., 2012). This is visualized in the fifth column of Fig. 1, where the concentrations of structural impurities in these samples predominantly plot in the white area, close to or below the HPQ concentrations threshold (stepped boundary between white and grey areas in the fifth column of Fig. 1; <50 μg g^{-1} in total). Furthermore, two of these quartzes (GA2 and GULL) are confidently devoid of feldspar inclusions, and thus serve as a baseline for uncontaminated quartz OSL signals, to be compared in Section 4.3 to that from HPQ with known presence of feldspar microinclusions (DRAG).

As already mentioned before, none of these HPQ samples possess a dominant 'fast' BLSL component (Fig. 2). Instead, an apparently universal occurrence of an ultrafast component (σ~5×10^{-16} cm^2; cf. Jain et al., 2008) can be noted. We now turn to look at the pulsed luminescence behaviour (columns 3 and 4 in Fig. 1) from these samples. The TR-BLSL decay curve (solid blue line

(in web version) in column 3) of GA2, the purest quartz in our dataset, consists of a single decaying exponential, peaking around the familiar ~37 μs lifetime (Ankjærgaard et al., 2010b), and prominently apparent in sample WIDG8 (containing ~500 μg g^{-1} of trace elements, i.e. ten times above the HPQ threshold). Although in all the three HPQ samples the natural TR-BLSL lifetime is dominated by the ~37 μs component, significantly shorter lifetimes (~2 μs and ~0.04 μs) become discernible as quartz chemistry progressively degrades in DRAG and GULL, respectively. Note that in sample KTB218A (~1000 μg g^{-1} of trace elements), these short recombination lifetimes predominate, while the ~37 μs recombination centre is hardly present at all. The TR-BLSL behaviour in KTB218A is almost identical to that exhibited by the feldspar sample FK981014, which has a broad and multimodal distribution of TR-OSL lifetimes, in sharp contrast to that of pure (GA2) or well-sensitized quartz (WIDG8). To summarize, it may be inferred that TR-BLSL lifetime components below or exceeding ~37 μs are directly related to intrinsic impurities and/or inclusions of feldspar (DRAG, KTB218A) or other minerals (GULL) within quartz.

4.3. IRSL from quartz

Although it has been suggested that trace elements in quartz, such as the $Al^{3+}(alkali)^{+}$ complex, may be responsible for genuine IRSL signals arising from the quartz lattice itself (Godfrey-Smith and Cada, 1996), such signals are orders of magnitude weaker than typical IRSL from feldspar. This is convincingly demonstrated by the total absence of any detectable IRSL in GA2 and GULL, which are confidently devoid of feldspar inclusions, compared to the bright natural IRSL signal in DRAG (red solid (in web version) curves in column 1 of Fig. 1), known to contain rare microinclusions of albite and biotite (~0.02% by weight). This relative brightness of the IRSL is quantified by the IRSL/BLSL ratio, which for sample DRAG amounts to 66%. In comparison, the IRSL/BLSL ratios of both GA2 and GULL are well below 1%.

Although high IRSL/BLSL ratios can detect even minute amounts of feldspar, low IRSL/BLSL ratios do not necessarily confirm its absence. For example, the IRSL/BLSL of WIDG8 is <0.1%, yet our LA-ICP-MS measurements made on a 100 polished single grains have demonstrated the presence of feldspar and zircon inclusions, among others. In this case, the IRSL from the inclusions, although present, is several orders of magnitude lower that the BLSL from the host quartz, and is thus not posing a signal interference problem.

The IRSL/BLSL ratios of NWE1, K0587, TWNG6 and KTB218A are all significantly above the recommended 10% threshold (Buylaert et al., 2008). Note that reduced grain size (4–11 μm in NWE1) does not seem to reduce this contamination, even though one would generally expect fewer inclusions in quartz grains of such small size. Note that IRSL/BLSL ratios in common bedrock quartz may fall either above or below that of pure feldspar, which for the particular sample FK981014 is 140%. The highest IRSL/BLSL ratio (609%) is exhibited by sample KTB218A. Note, however, that from the perspective of simple stoichiometric mixing between pure quartz (GA2) and pure feldspar (FK981014) end members (column 5 in Fig. 1), only ~1% by weight of feldspar is sufficient to give rise to such an overwhelmingly high IRSL/BLSL ratio.

4.4. Sensitization of quartz by annealing

Despite the undesirable characteristics of the natural OSL signals in the majority of the studied bedrock quartzes, these characteristics significantly improve after a laboratory thermal annealing at 650 °C for 10 min. The CW- and TR-OSL curves of annealed GA2, DRAG, GULL and KTB218A are shown as dashed blue and red lines (in web version) on columns 1–4 in Fig. 1. The result of the annealing is twofold, affecting both the CW-OSL and TR-OSL curve shapes. In CW-BLSL, the annealing removes the ultrafast component (present in all the HPQ and the KTB218A samples), and generally enhances the fast component, thereby reducing the IRSL/BLSL ratio (e.g. from 66% to 7% in DRAG). In TR-BLSL, the annealing removes the short recombination lifetimes (present in DRAG, GULL and KTB218A), and enhances the ~37 μs recombination to >95% in GULL and DRAG, and from 4% to 14% in KTB218A.

5. Applicability of luminescence signals for thermochronometry

Regardless of whether a target OSL signal can or cannot be extracted, we now proceed to address a purely theoretical consideration of whether this signal is or is not suitable to solve a posed thermochronometric question. To go beyond the treatment presented by Li and Li (2012), we address the universal phenomenon of OSL signal saturation (cf. Grün, 2001) merely as a special case of a more general problem (i.e. inability to distinguish signals from their predictable environmental steady-state). While the analysis of other saturation-limited trapped-charge methods such as quartz thermoluminescence (TL; see Tsuchiya et al., 2000) and electron spin resonance (ESR; see Grün et al., 1999) is analogous, their treatment is outside of the scope of the current paper.

In thermochronometry, one is primarily interested in determining the timing and rate of heating or cooling histories of geological formations (Reiners and Ehlers, 2005). For cooling, we consider bedrock, progressively brought to the surface of Earth by erosion, and evolved from high temperatures where nearly all luminescence signals are reset by heat. For heating, we consider sediments, whose luminescence signals were optically reset by sunlight prior to burial in a sedimentary basin. Therefore, the concentration in all of our considered geological scenarios will conveniently evolve from zero ($n_0/N = 0$), providing an easy comparison between the cooling and the heating environments. In our calculations, we further adopt $\dot{D} = 2$ Gy ka^{-1} as a representative rate of background radioactivity in typical bedrock environments, and use literature values of the kinetic parameters E [eV], s [s^{-1}] and D_0 [Gy] as listed in Table 2.

Fig. 3a shows the evolution of the fractional trap filling n/N (see Section 3.3) of the fast OSL component as a function of the instantaneous temperature T, for a cooling (dashed line) and a heating (dotted line) scenario, both at a linear rate of $dT/dt = 100$ °C Ma^{-1}. For comparison, we also show the fractional trap filling at steady-state $(n/N)_{SS}$, attained after an infinite isothermal holding at any particular temperature T (solid gray line). Although the shown cooling/heating rate in Fig. 3a is on the higher end of geologically feasible values (Wright, 1980; Reiners and Brandon, 2006), it is nevertheless a reasonable choice for OSL systems, as a slower rate may often result in transient n/N concentrations that are indiscernible from the environmental steady-state $(n/N)_{SS}$ conditions. Also note, that while cooling leads to a monotonic increase in concentration, a heating scenario is characterised by

Table 2
Arrhenius parameters and characteristic doses of various quartz OSL signals.

Component	E [eV]	s [s^{-1}]	D_0 [Gy]	Reference
OSL fast	1.74	8.9×10^{13}	190	Singarayer and Bailey, 2003
OSL medium	1.80	1.5×10^{13}	258	
OSL slow	2.02	6.9×10^{14}	250	
TT-OSL 1 kGy	1.46	6.7×10^{11}	1000	Adamiec et al., 2010;
TT-OSL 10 kGy			10000	Duller and Wintle, 2012
VSL A	1.92	5×10^{15}	3200	Ankjærgaard et al., 2013
VSL B	1.92	3×10^{15}	1200	

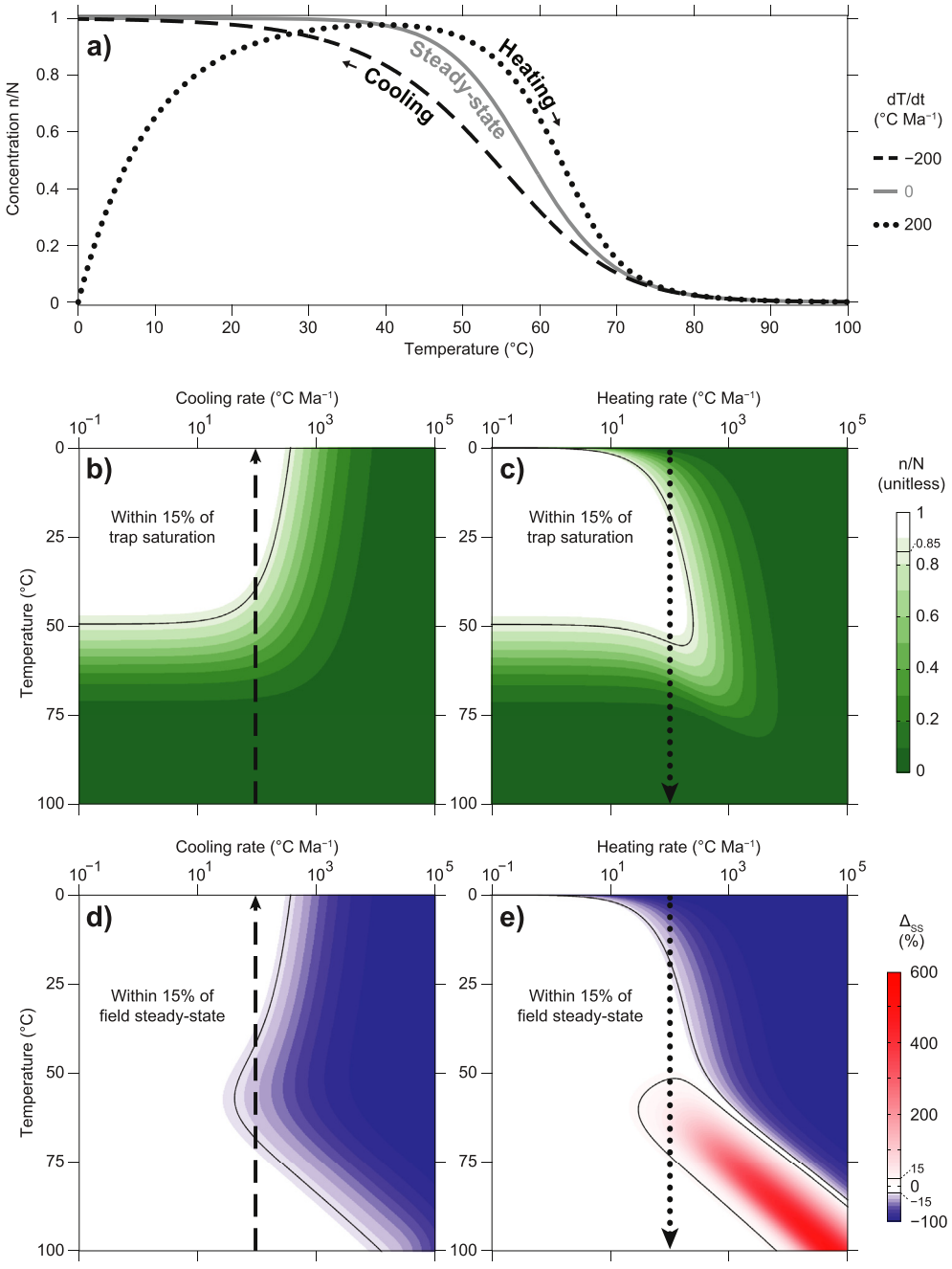

Fig. 3. a) Evolution of the relative trap filling n/N of the fast OSL component in a set of representative linear cooling (dashed), heating (dotted) and thermal steady-state (solid grey) scenarios. b-c) shaded contours of n/N as a function of different cooling (b) and heating (c) rates. d-e) relative disequilibrium (see text) as a function of different cooling (d) and heating (e) rates. White areas in b-d represent geological conditions in which precise age determination (b–c) or reconstruction of transient processes (d–e) is improbable due to current methodological uncertainties.

initial concentration growth (for T<45 °C in Fig. 3a) followed by its subsequent decay (for T>45 °C in Fig. 3a).

The shaded colour map in Fig. 3b, c corresponds to contours of n/N (dark green (in the web version) is 0, white is 1) of the fast OSL component, as a function of various linear cooling (Fig. 3b) and heating (Fig. 3c) rates. The two previously discussed scenarios of cooling and heating at 100 °C Ma^{-1} (in Fig. 3a) are repeated here with identically dashed (Fig. 3b) and dotted (Fig. 3c) black arrowed lines. The bright white area on the upper left corners of Fig. 3b–c (enclosed by a solid thin black line) corresponds to conditions where the fast OSL trap is within 15% of its saturation level (i.e. more than 85% of the electron traps are occupied, n/N>0.85). Under such conditions, it is advisable to report only a minimum age, due to the presently large uncertainty regarding the dose response bordering system saturation (Wintle and Murray, 2006).

Fig. 3b demonstrates that cooling at a rapid rate of 100 °C Ma^{-1} from 100 °C to 0 °C produces a near-saturation trap filling of $n/N = 0.89$, i.e. within <15% of a fully occupied system. The associated apparent age of 209 ka (Eq. A.4 in Guralnik et al., 2013) gives only a minimum age estimate, since even much longer irradiation histories may end up with rather comparable concentrations.

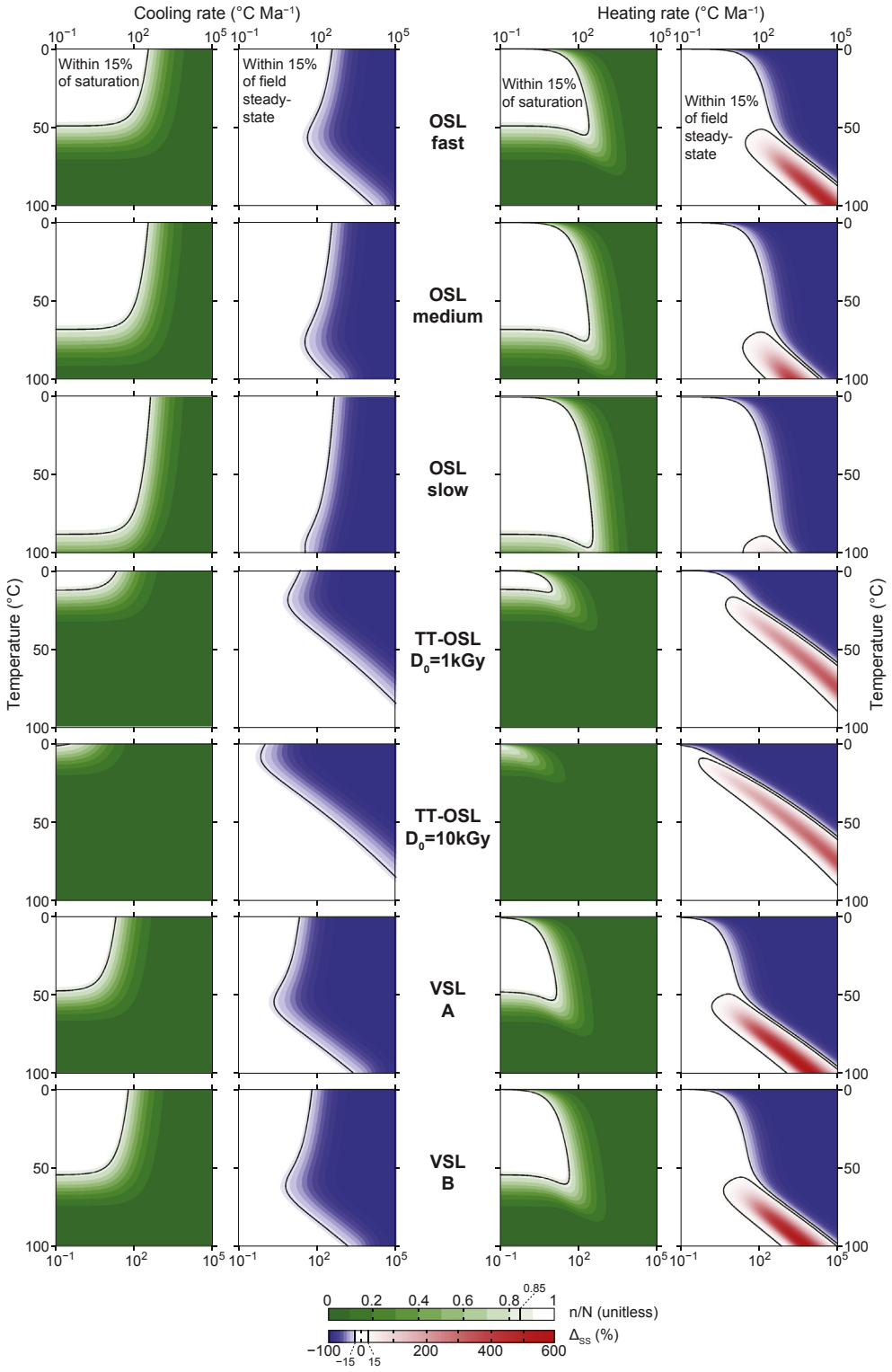

Fig. 4. Comparison of trap filling (columns 1 and 3) and relative disequilibrium conditions (columns 2 and 4) as explained in Fig. 3, for various OSL signals encountered in the literature (Table 2) and subjected to linear cooling (columns 1–2) and heating (columns 3–4) scenarios.

Alternatively, if the former cooling history terminates at 50 °C, or if the same sample cools from 100 °C to 0 °C at a rate of 750 °C Ma^{-1}, the above scenarios will both evolve to a final concentration of $n/N = 0.62$. The corresponding apparent ages (107 ka and 92 ka, respectively) may then be successfully converted to their respective paleotemperatures through the revised formula for closure temperature (Guralnik et al., 2013). Conversely, to reconstruct rock heating scenarios related to sedimentary burial (Fig. 3c), a distribution of cooling ages with depth is typically required (cf. Green et al., 1989). Note that a depositional profile is characterised by stratigraphic ages (concentrations) in the top of the profile, and thermally reset ages (concentrations) in its bottom.

Whether in saturation or not, a measured n/N yields valuable information. In order to discern whether a given n/N reflects a stationary holding temperature or a transient cooling/heating process, we compare instantaneous n/N values in Fig. 3b, c to their steady-state values $(n/N)_{SS}$ at thermal equilibrium (Eq. A.9b in Guralnik et al., 2013). We define Δ_{SS} as the percent deviation from steady-state concentration, i.e. $\Delta_{SS} = [(n/N)-(n/N)_{SS}]/(n/N)_{SS}$. Positive and negative values of Δ_{SS} correspond to higher-than-steady-state (red shades (in web version) in Fig. 3e) or lower-than-steady-state (blue shades(in web version) in Fig. 3d, e) concentrations, while $\Delta_{SS} = 0$ strictly implies thermal equilibrium. The white area in Fig. 3d, e corresponds to $|\Delta_{SS}|<0.15$, i.e. regions, where transient concentrations are within 15% of their environmental steady-state levels. Since saturation (white area on Fig. 3b, c) is just a special case of steady-state (white area on Fig. 3d, e), it is evident that the low-temperature regions (<50 °C) of the white areas in Fig. 3d, e are identical to those of in Fig. 3b, c, and in fact contain the former. To continue the previous example, we again consider the two former scenarios of cooling, one from 100 °C to 50 °C at 100 °C Ma^{-1}, and the other from 100 °C to 0 °C at 750 °C Ma^{-1}, both evolving to a final concentration of $n/N = 0.62$. The respective $(n/N)_{SS}$ at 50 °C and 0 °C are 0.84 and 1, and the corresponding Δ_{SS} are thus $(0.62-0.84)/0.84 = -26\%$ and $(0.62-1)/1 = -38\%$. This indicates that the observed $n/N = 0.62$ in both situations is tens of percent away from the anticipated steady-state concentrations at these temperatures, and thus may be confidently used to infer the corresponding rates of cooling. Yet for a cooling from 100 °C to 50 °C at 10 °C Ma^{-1}, the final $n/N = 0.81$ is far too close to its steady-state value of $(n/N)_{SS} = 0.84$ to allow inferring the cooling rate, even though the sample is below the level of saturation (i.e. <0.85). The consequence is that an observed $n/N = 0.81$ at 50 °C cannot be confidently translated to a process rate, but instead reflects the near steady-state conditions achieved after prolonged storage at ~50 °C.

Fig. 3 shows, that for typical surface temperatures (<25 °C) and process rates ($|dT/dt|$<100 °C Ma^{-1}) on Earth, the fast OSL component would be more often found in either saturation (Fig. 3b, c) or in field steady-state (Fig. 3d, e) than in detectably transient conditions indicative of process rates. To explore the possible existence of more favourable OSL signals in quartz, Fig. 4 compares the saturation and steady-state fields across the fast, medium and slow components of quartz BLSL, alongside the developmental TT-OSL and VSL protocols (Wang et al., 2006; Duller and Wintle, 2012; Ankjærgaard et al., 2013). It can be seen that the characteristics of the medium (row 2) and the slow (row 3) OSL components are even less favourable than those of the fast OSL component (row 1). Quite promising characteristics are found in the TT-OSL signal, although the presently debated D_0 of TT-OSL (1 kGy in row 4 vs. 10 kGy in row 5) needs further clarification (see Duller and Wintle, 2012) to allow a coherent thermochronological interpretation. Lastly, we include the two violet stimulated signals from quartz (rows 6–7 in Fig. 4), that too exhibit D_0 in the kGy range (Jain, 2009; Ankjærgaard et al., 2013), and thus appear to have a similar potential to the TT-OSL signal.

As a concluding remark, it must be acknowledged that the signal behaviours summarized in Fig. 4 correspond to literature values only (Table 2). While representative, more favourable conditions such as low environmental radioactivity, high saturation dose, or low thermal stability may nevertheless enable a successful conversion of an OSL signal into a process rate, even where predicted here as improbable.

6. Discussion

In this study we have used three diagnostic tools to investigate whether a quartz sample exhibits desirable luminescence characteristics for standard OSL dating (Wintle and Murray, 2006). These are (i) the photoionisation cross section of the electron trap(s) giving rise to the CW-BLSL signal, (ii) the IRSL/BLSL ratio, and (iii) the TR-BLSL relaxation lifetime(s) of the luminescence centres. Collectively, these criteria represent the minimal quality control that should be applied to any OSL-thermochronometric sample, in light of the generally problematic OSL characteristics of bedrock quartz. Based on the nine investigated samples, the natural 'fast' OSL component of crystalline bedrock quartz is frequently unsensitised. Instead, it is often dominated by the ultrafast component in the CW-BLSL signal (Jain et al., 2008), and by short recombination lifetimes in the TR-BLSL (Chithambo et al., 2007); both these familiar features obscure the separation of the desired signal from the calibrated dosimetric trap, and are thus advised to be instrumentally removed before (Goble and Rittenour, 2006) and during (Thomsen et al., 2008a; Ankjærgaard et al., 2010b) the optical stimulation, respectively. Additionally, bedrock quartz often exhibits high IRSL/BLSL ratios, characteristic of signal contamination by feldspar, and reported to bias age estimates (Buylaert et al., 2008). Such poor quality of the natural OSL signals, familiar from sedimentary-immature environments (cf. Preusser et al., 2009), can be significantly improved by laboratory annealing (Bøtter-Jensen et al., 1993), which reduces the unwanted components in the CW-BLSL and TR-BLSL signals and decreases the IRSL/BLSL ratio, thus making the quartz signal comparable to that employed in standard OSL dating. This laboratory annealing process probably imitates the sensitization of recombination centres occurring naturally in the sedimentary environment due to repeated cycles of dosing and light exposure (Moska and Murray, 2006). However, such high-temperature laboratory pretreatment would remove the desirable natural signal, and thus currently precludes a successful dating of the originally insensitive sample.

To further demonstrate the typical problems of OSL from crystalline (i.e. magmatic and metamorphic) quartz, it is instructive to consider the luminescence characteristics of the chemically-purest samples (HPQ) in our dataset. Most strikingly, even the smallest amount of feldspar contamination (0.02% by weight in DRAG) can give rise to an unacceptably high IRSL/BLSL ratio (66% in DRAG), thus potentially compromising a reliable dosimetry of that sample (Buylaert et al., 2008). Since macro-scale occurrence of HPQ in nature is rare, one may expect that such anomalously high IRSL/BLSL ratios in crystalline quartz would be the rule, rather than the exception, in average crystalline bedrock environments. Furthermore, in the unlikely case of zero feldspar contamination (e.g. samples GA2 and GULL), the relative contribution of the fast component (only ~9% in GA2) and the ~37 μs recombination centre (only ~32% in GULL) may be so insignificant as to seriously complicate their reliable extraction and ultimately, their interpretation. In light of the above, we suggest that the quantitative results obtained in recent OSL-thermochronology studies (Herman et al., 2010; De Sarkar et al., 2013) ought to be addressed with caution. It is also important to note here, that the absence of a fast OSL component in a natural signal does not necessarily imply that the associated electron trap of interest (E~1.8 eV, s~10^{14} s^{-1}, D_0~150 Gy and σ~2.60×10^{-17} cm^2, see Table 2) is not present in the natural system. Instead, it might rather reflect the insensitivity of the associated recombination centres (Preusser et al., 2009), and thus potentially enable a signal extraction by another, yet undiscovered, method.

In contrast to the various crystalline environments, the studied quartzes from the sedimentary or low-grade metamorphic context exhibited satisfactory OSL behaviour, all displaying a dominant fast component and a relatively low IRSL/BLSL ratio. From the limited dataset, it may be speculated that the threshold metamorphic temperature, below which bedrock quartz may preserve the

luminescence characteristics of its unconsolidated parent sediment, is ~380 °C, and close to the 325 °C thermoluminescence peak associated with the dosimetric trap (Wintle and Murray, 1997). While ~380 °C may not be a universal threshold for bedrock quartz properties, (i) it falls in line with far more frequent reports on insensitive (Preusser et al., 2009; references therein; Sohbati et al., 2011; Jeong and Choi, 2012; Rittenour et al., 2012; Fuchs et al., 2013) rather than sensitive (Sawakuchi et al., 2011) quartz from crystalline bedrock environments, (ii) it suggests that the outlined signal quality control is essential (cf. Preusser et al., 2009) to any future application of quartz OSL-thermochronology, and (iii) one may generally expect better quartz OSL characteristics in subsurface samples from subsiding sedimentary basins, rather than in surface samples from exhuming crystalline terrains.

Even if present, the fast OSL component in quartz has a rather low saturation dose, which generally limits its thermochronometric capability to infer transient processes only to very rapid (>100 °C Ma^{-1}) cooling or heating scenarios. When the regional thermal processes occur at slower rates, quartz OSL would tend to be in field-steady state and thus enable inferring the ambient thermal conditions rather than cooling or heating rates. Considering existing alternatives to the fast OSL component in quartz, its medium and slow components have even narrower applicability fields, due to their higher thermal activation energies. Currently developmental protocols (TT-OSL and VSL) which extend the typical OSL dating range via higher saturation doses, appear to be better-suited to infer typical geological processes in the range of $10^{-1} - 10^{2}$ °C Ma^{-1}. Finally, although other trapped-charge techniques (e.g. quartz TL and ESR) are known to be applicable to thermochronometry, their evaluation via the presented theoretical framework remains outside of the scope of the current paper.

As a final point, the brightness of IRSL from feldspar extracts (e.g. Sohbati et al., 2011) or inclusions in quartz (e.g. Huntley et al., 1993) suggests that feldspar IRSL might be a more straightforward target luminescence signal for extraction in crystalline bedrock environments. Although feldspar IRSL suffers from athermal loss pathways, major advancements in both fading correction (Kars et al., 2008) and extraction of non-fading signals (Thomsen et al., 2008b; Li and Li, 2011; Buylaert et al., 2012b) suggests that these signals may be a better alternative for OSL-thermochronometry than the frequently encountered insensitive OSL signals from quartz.

7. Conclusions

This study presents a set of standard diagnostic tools to evaluate the quality of luminescence signals of diverse bedrock quartz against that of a benchmark sedimentary quartz (WIDG8). These include (i) the photoionisation cross section (ii) the relative intensity of the IRSL and BLSL signals, and (ii) the TR-BLSL recombination lifetime. We find desirable OSL characteristics only in rocks that have not been subjected to metamorphic temperatures exceeding ~380 °C, such as mature sediments or low-grade metapelites ($n = 3$). All higher-grade metamorphic and magmatic quartz ($n = 6$) displayed anomalous quartz OSL characteristics, currently avoided in dating. While such characteristics can be improved by high-temperature laboratory annealing, the latter removes the natural luminescence signal and hence precludes the objective of dating. Even if present in a sample, the fast OSL component may be expected to be found either in saturation or in field steady-state (for typical surface temperatures and common geological cooling/heating rates), and is therefore less advantageous compared to developmental OSL signals with either a lower thermal stability or a higher saturation limit. Finally, to ensure full methodological transparency of OSL-thermochronometric datasets, we stress that the proper measurement and documentation of the power density P of the optical stimulation source [W cm^{-2}], and of the relevant kinetic parameters of the targeted electron trap (E, s, and D_0), has to become obligatory in application studies, rather than optional.

Acknowledgements

This manuscript has significantly benefitted and broadened its scope thanks to the thorough and stimulating reviews by an anonymous reviewer and J. Durcan. We thank Guiditta Fellin for guidance in mineral separation of sample KTB218A. This work was supported by the Swiss National Foundation grant 200021–127127. CA was financed by Technology Foundation STW (grant number STW.10502) and NWO VENI, and TSW acknowledges support from the National Science Council of Taiwan (grant number NSC97-2116-M-002-017-MY3).

References

Adamiec, G., Duller, G.A.T., Roberts, H.M., Wintle, A.G., 2010. Improving the TT-OSL SAR protocol through source trap characterisation. Radiat. Meas. 45, 768–777.
Ankjærgaard, C., Denby, P.M., Murray, A.S., Jain, M., 2008. Charge movement in grains of quartz studied using exo-electron emission. Radiat. Meas. 43, 273–277.
Ankjærgaard, C., Jain, M., Hansen, P.C., Nielsen, H.B., 2010a. Towards multi-exponential analysis in optically stimulated luminescence. J. Phys. D. Appl. Phys. 43, 195501.
Ankjærgaard, C., Jain, M., Thomsen, K.J., Murray, A.S., 2010b. Optimising the separation of quartz and feldspar optically stimulated luminescence using pulsed excitation. Radiat. Meas. 45, 778–785.
Ankjærgaard, C., Jain, M., Wallinga, J., 2013. Towards dating Quaternary sediments using the quartz Violet Stimulated Luminescence (VSL) signal. Quat. Geochronol. 18, 99–109.
Bailey, R.M., Smith, B.W., Rhodes, E.J., 1997. Partial bleaching and the decay form characteristics of quartz OSL. Radiat. Meas. 27, 123–136.
Bailiff, I.K., 2000. Characteristics of time-resolved luminescence in quartz. Radiat. Meas. 32, 401–405.
Baril, M.R., 2004. Emission and excitation spectra of feldspar inclusions within quartz. Radiat. Meas. 38, 87–90.
Beyssac, O., Simoes, M., Avouac, J.P., Farley, K.A., Chen, Y.G., Chan, Y.C., Goffé, B., 2007. Late Cenozoic metamorphic evolution and exhumation of Taiwan. Tectonics 26, TC6001.
Bøtter-Jensen, L., 1997. Luminescence techniques: instrumentation and methods. Radiat. Meas. 27, 749–768.
Bøtter-Jensen, L., Jungner, H., Mejdahl, V., 1993. Recent developments of OSL techniques for dating quartz and feldspars. Radiat. Prot. Dosim. 47, 643–648.
Bøtter-Jensen, L., McKeever, S.W.S., Wintle, A.G., 2003. Optically Stimulated Luminescence Dosimetry. Elsevier, Amsterdam.
Buylaert, J.P., Huot, S., Murray, A.S., Van den Haute, P., 2011. Infrared stimulated luminescence dating of an Eemian (MIS 5e) site in Denmark using K-feldspar. Boreas 40, 46–56.
Buylaert, J.P., Jain, M., Murray, A.S., Thomsen, K.J., Lapp, T., 2012a. IR-RF dating of sand-sized K-feldspar extracts: a test of accuracy. Radiat. Meas. 47, 759–765.
Buylaert, J.P., Jain, M., Murray, A.S., Thomsen, K.J., Thiel, C., Sohbati, R., 2012b. A robust feldspar luminescence dating method for Middle and Late Pleistocene sediments. Boreas 41, 435–451.
Buylaert, J.P., Murray, A.S., Thomsen, K.J., Jain, M., 2009. Testing the potential of an elevated temperature IRSL signal from K-feldspar. Radiat. Meas. 44, 560–565.
Buylaert, J.P., Murray, A.S., Vandenberghe, D., Vriend, M., De Corte, F., 2008. Optical dating of Chinese loess using sand-sized quartz: establishing a time frame for Late Pleistocene climate changes in the western part of the Chinese Loess Plateau. Quat. Geochronol. 3, 99–113.
Chithambo, M.L., Galloway, R.B., 2000a. A pulsed light-emitting-diode system for stimulation of luminescence meas. Sci. Technol. 11, 418.
Chithambo, M.L., Galloway, R.B., 2000b. Temperature dependence of luminescence time-resolved spectra from quartz. Radiat. Meas. 32, 627–632.
Chithambo, M.L., Preusser, F., Ramseyer, K., Ogundare, F.O., 2007. Time-resolved luminescence of low sensitivity quartz from crystalline rocks. Radiat. Meas. 42, 205–212.
Choi, J.H., Duller, G.A.T., Wintle, A.G., 2006. Analysis of quartz LM-OSL curves. Anc. TL 24, 9–20.
Christodoulides, C., Ettinger, K.V., Fremlin, J.H., 1971. The use of TL glow peaks at equilibrium in the examination of the thermal and radiation history of materials. Mod. Geol. 2, 275–280.
Daniels, F., Boyd, C.A., Saunders, D.F., 1953. Thermoluminescence as a research tool. Science 117, 343–349.
De Sarkar, S., Mathew, G., Pande, K., Chauhan, N., Singhvi, A.K., 2013. Rapid denudation of higher Himalaya during late Pliestocence, evidence from OSL thermochronology. Geochronometria 40, 304–310.

Dehnert, A., Lowick, S.E., Preusser, F., Anselmetti, F.S., Drescher-Schneider, R., Graf, H.R., Heller, F., Horstmeyer, H., Kemna, H.A., Nowaczyk, N.R., Züger, A., Furrer, H., 2012. Evolution of an overdeepened trough in the northern Alpine Foreland at Niederweningen, Switzerland. Quat. Sci. Rev. 34, 127–145.
Duller, G.A.T., Wintle, A.G., 2012. A review of the thermally transferred optically stimulated luminescence signal from quartz for dating sediments. Quat. Geochronol. 7, 6–20.
Duller, G.A.T., 2003. Distinguishing quartz and feldspar in single grain luminescence measurements. Radiat. Meas. 37, 161–165.
Durcan, J.A., Duller, G.A.T., 2011. The fast ratio: a rapid measure for testing the dominance of the fast component in the initial OSL signal from quartz. Radiat. Meas. 46, 1065–1072.
Durrani, S.A., Khazal, K.A.R., Ali, A., 1977. Temperature and duration of the shadow of a recently-arrived lunar boulder. Nature 266, 411–415.
Fuchs, M.C., Böhlert, R., Krbetschek, M., Preusser, F., Egli, M., 2013. Exploring the potential of luminescence methods for dating Alpine rock glaciers. Quat. Geochronol. 18, 17–33.
Goble, R.J., Rittenour, T.M., 2006. A linear modulation OSL study of the unstable ultrafast component in samples from Glacial Lake Hitchcock, Massachusetts, USA. Anc. TL 24, 37–46.
Godfrey-Smith, D.I., Cada, M., 1996. IR stimulation spectroscopy of plagioclase and potassium feldspars, and quartz. Radiat. Prot. Dosim. 66, 379–385.
Götze, J., 2012. Classification, mineralogy and industrial potential of SiO_2 minerals and rocks. In: Quartz: Deposits, Mineralogy and Analytics. Springer, Berlin Heidelberg, pp. 1–27.
Götze, J., Plötze, M., Graupner, T., Hallbauer, D.K., Bray, C.J., 2004. Trace element incorporation into quartz: a combined study by ICP-MS, electron spin resonance, cathodoluminescence, capillary ion analysis, and gas chromatography. Geochim. Cosmochim. Acta 68, 3741–3759.
Grapes, R., Watanabe, T., 1992. Metamorphism and uplift of Alpine schist in the Franz Josef–Fox Glacier area of the Southern Alps, New Zealand. J. Metam. Geol. 10, 171–180.
Green, P.F., Duddy, I.R., Laslett, G.M., Hegarty, K.A., Gleadow, A.W., Lovering, J.F., 1989. Thermal annealing of fission tracks in apatite 4. Quantitative modelling techniques and extension to geological timescales. Chem. Geol. Isot. Geosci. Sect. 79, 155–182.
Grün, R., 2001. Trapped charge dating (ESR, TL, OSL). In: Brothwell, D.R., Pollard, A.M. (Eds.), Handbook of Archaeological Sciences. John Wiley & Sons Inc., West Sussex, England, pp. 47–62.
Grün, R., Tani, A., Gurbanov, A., Koshchug, D., Williams, I., Braun, J., 1999. A new method for the estimation of cooling and rates using paramagnetic centers in quartz: a case study on the Eldzhurtinskiy Granite, Caucasus. J. Geophys. Res. 104, 17531–17549.
Guralnik, B., Jain, M., Herman, F., Paris, R.B., Harrison, T.M., Murray, A.S., Valla, P.V., Rhodes, E.J., 2013. Effective closure temperature in leaky and/or saturating thermochronometers. Earth Planet. Sci. Lett. 384, 209–218.
Herman, F., Rhodes, E.J., Braun, J., Heiniger, L., 2010. Uniform erosion rates and relief amplitude during glacial cycles in the Southern Alps of New Zealand, as revealed from OSL-thermochronology. Earth Planet. Sci. Lett. 297, 183–189.
Horch, R.A., Gochberg, D.F., Nyman, J.S., Does, M.D., 2012. Clinically compatible MRI strategies for discriminating bound and pore water in cortical bone. Magn. Res. Med. 68, 1774–1784.
Horch, R.A., Gore, J.C., Does, M.D., 2011. Origins of the ultrashort-T21H NMR signals in myelinated nerve: a direct measure of myelin content? Magn. Res. Med. 66, 24–31.
Houtermans, F.G., Jäger, E., Schön, M., Stauffer, H., 1957. Messungen der thermolumineszenz als mittel zur untersuchung der thermischen und der strahlungsgeschichte von natürlichen mineralien und gesteinen. Ann. Phys. 20, 283–292.
Huntley, D.J., Hutton, J.T., Prescott, J.R., 1993. Optical dating using inclusions within quartz grains. Geology 21, 1087–1090.
Jain, M., 2009. Extending the dose range: probing deep traps in quartz with 3.06 eV photons. Radiat. Meas. 44, 445–452.
Jain, M., Choi, J.H., Thomas, P.J., 2008. The ultrafast OSL component in quartz: origins and implications. Radiat. Meas. 43, 709–714.
Jeong, G.Y., Choi, J.H., 2012. Variations in quartz OSL components with lithology, weathering and transportation. Quat. Geochronol. 10, 320–326.
Johnson, N.M., 1963. Thermoluminescence in contact metamorphosed limestone. J. Geol. 71, 596–616.
Kars, R.H., Wallinga, J., Cohen, K.M., 2008. A new approach towards anomalous fading correction for feldspar IRSL dating—tests on samples in field saturation. Radiat. Meas. 43, 786–790.
Kidder, S., Avouac, J.P., Chan, Y.C., 2013. Application of titanium-in-quartz thermobarometry to greenschist facies veins and recrystallized quartzites in the Hsüehshan range, Taiwan. Solid Earth 4, 1–21.
Krbetschek, M.R., Götze, J., Dietrich, A., Trautmann, T., 1997. Spectral information from minerals relevant for luminescence dating. Radiat. Meas. 27, 695–748.
Kronz, A., van den Kerkhof, A.M., Müller, A., 2012. Analysis of low element concentrations in quartz by electron microprobe. In: Quartz: Deposits, Mineralogy and Analytics. Springer, Berlin Heidelberg, pp. 191–217.
Lapp, T., Jain, M., Ankjærgaard, C., Pirtzel, L., 2009. Development of pulsed stimulation and Photon Timer attachments to the Risø TL/OSL reader. Radiat. Meas. 44, 571–575.
Li, B., Li, S.-H., 2011. Luminescence dating of K-feldspar from sediments: a protocol without anomalous fading correction. Quat. Geochronol. 6, 468–479.
Li, B., Li, S.-H., 2012. Determining the cooling age using luminescence thermochronology. Tectonophysics 580, 242–248.
Monnier, F., 1982. Thermal diagenesis in the Swiss molasse basin: implications for oil generation. Can. J. Earth Sci. 19, 328–342.
Moska, P., Murray, A.S., 2006. Stability of the quartz fast-component in insensitive samples. Radiat. Meas. 41, 878–885.
Müller, A., Ihlen, P.M., Wanvik, J.E., Flem, B., 2007. High-purity quartz mineralisation in kyanite quartzites, Norway. Mineral. Deposita 42, 523–535.
Müller, A., Koch-Müller, M., 2009. Hydrogen speciation and trace element contents of igneous, hydrothermal and metamorphic quartz from Norway. Mineral. Mag. 73, 569–583.
Müller, A., Wanvik, J.E., Ihlen, P.M., 2012. Petrological and chemical characterisation of high-purity quartz deposits with examples from Norway. In: Quartz: Deposits, Mineralogy and Analytics. Springer, Berlin Heidelberg, pp. 71–118.
Murray, A.S., Buylaert, J.P., Thomsen, K.J., Jain, M., 2009. The effect of preheating on the IRSL signal from feldspar. Radiat. Meas. 44, 554–559.
Murray, A.S., Olley, J.M., 2002. Precision and accuracy in the optically stimulated luminescence dating of sedimentary quartz: a status review. Geochronometria 21, 1–16.
Murray, A.S., Roberts, R.G., Wintle, A.G., 1997. Equivalent dose measurement using a single aliquot of quartz. Radiat. Meas. 27, 171–184.
Murray, A.S., Wintle, A.G., 1999. Isothermal decay of optically stimulated luminescence in quartz. Radiat. Meas. 30, 119–125.
O'Connor, S., 1999. 30,000 Years of Aboriginal Occupation, Kimberly, North West Australia, vol. 14. ANH Publications.
Pagonis, V., Ankjærgaard, C., Murray, A.S., Jain, M., Chen, R., Lawless, J., Greilich, S., 2010. Modelling the thermal quenching mechanism in quartz based on time-resolved optically stimulated luminescence. J. Lumin. 130, 902–909.
Pagonis, V., Chithambo, M.L., Chen, R., Chruścińska, A., Fasoli, M., Li, S.H., Martini, M., Ramseyer, K., 2014a. Thermal dependence of luminescence lifetimes and radioluminescence in quartz. J. Lumin. 145, 38–48.
Pagonis, V., Phan, H., Goodnow, R., Rosenfeld, S., Morthekai, P., 2014b. Mathematical characterization of continuous wave infrared stimulated luminescence signals (cw-IRSl) from feldspars. J. Lumin. 154, 362–368.
Poolton, N.R.J., Botter-Jensen, L., Johnsen, O., 1997. A search for IRSL-active dosemeters with enhanced sensitivity: a spectroscopic survey. Radiat. Meas. 27, 279–290.
Preusser, F., Chithambo, M.L., Götte, T., Martini, M., Ramseyer, K., Sendezera, E.J., Susino, G.J., Wintle, A.G., 2009. Quartz as a natural luminescence dosimeter. Earth Sci. Rev. 97, 184–214.
Prokein, J., Wagner, G.A., 1994. Analysis of thermoluminescent glow peaks in quartz derived from the KTB-drill hole. Radiat. Meas. 23, 85–94.
Reiners, P.W., Brandon, M.T., 2006. Using thermochronology to understand orogenic erosion. Annu. Rev. Earth Pl. SC. 34, 419–466.
Reiners, P.W., Ehlers, T.A. (Eds.), 2005. Low-temperature Thermochronology: Techniques, Interpretations, and Applications. Rev. Mineral. Geochem, vol. 58, p. 622.
Reinhardt, J., 1997. Thermobarometry and P–T path of garnet–aluminosilicate-bearing gneisses from the KTB drill core (Continental Deep-Drilling Project, Germany). Geol. Rundsch. 86, S167–S183.
Rendell, H.M., Wood, R.A., 1994. Quartz sample pretreatments for TL/OSL dating: studies of TL emission spectra. Radiat. Meas. 23, 575–580.
Rittenour, T.M., 2008. Luminescence dating of fluvial deposits: applications to geomorphic, palaeoseismic and archaeological research. Boreas 37, 613–635.
Rittenour, T.M., Riggs, N.R., Kennedy, L.E., 2012. Application of single-grain OSL to date quartz xenocrysts within a basalt flow, San Francisco volcanic field, northern Arizona, USA. Quat. Geochronol. 10, 300–307.
Ronca, L.B., Zeller, E.J., 1965. Thermoluminescence as a function of climate and temperature. Am. J. Sci. 41, 118–121.
Sanderson, D.C.W., Clark, R.J., 1994. Pulsed photostimulated luminescence of alkali feldspars. Radiat. Meas. 23, 633–639.
Sawakuchi, A.O., Blair, M.W., DeWitt, R., Faleiros, F.M., Hyppolito, T., Guedes, C.C.F., 2011. Thermal history versus sedimentary history: OSL sensitivity of quartz grains extracted from rocks and sediments. Quat. Geochronol. 6, 261–272.
Short, M.A., Huntley, D.J., 1992. Infrared stimulation of quartz. Anc. TL 10, 19–21.
Singarayer, J.S., 2003. Linearly Modulated Optically Stimulated Luminescence of Sedimentary Quartz: Physical Mechanisms and Implications for Dating (Unpublished Ph D). University of Oxford.
Singarayer, J.S., Bailey, R.M., 2003. Further investigations of the quartz optically stimulated luminescence components using linear modulation. Radiat. Meas. 37, 451–458.
Smith, B.W., Rhodes, E.J., Stokes, S., Spooner, N.A., Aitken, M.J., 1990. Optical dating of sediments: initial quartz results from Oxford. Archaeometry 32, 19–31.
Sohbati, R., Murray, A.S., Jain, M., Buylaert, J.-P., Thomsen, K.J., 2011. Investigating the resetting of OSL signals in rock surfaces. Geochronometria 38, 249–258.
Stalder, M., Rozendaal, A., 2004. Apatite nodules as an indicator of depositional environment and ore genesis for the Mesoproterozoic Broken Hill-type Gamsberg Zn–Pb deposit, Namaqua Province, South Africa. Mineral. Dep. 39, 189–203.
Thomsen, K.J., Jain, M., Murray, A.S., Denby, P.M., Roy, N., Bøtter-Jensen, L., 2008a. Minimizing feldspar OSL contamination in quartz UV-OSL using pulsed blue stimulation. Radiat. Meas. 43, 752–757.
Thomsen, K.J., Murray, A.S., Jain, M., 2011. Stability of IRSL signals from sedimentary K-feldspar samples. Geochronometria 38, 1–13.

Thomsen, K.J., Murray, A.S., Jain, M., Bøtter-Jensen, L., 2008b. Laboratory fading rates of various luminescence signals from feldspar-rich sediment extracts. Radiat. Meas. 43, 1474–1486.
Tsuchiya, N., Suzuki, T., Nakatsuka, K., 2000. Thermoluminescence as a new research tool for the evaluation of geothermal activity of the Kakkonda geothermal system, Northeast Japan. Geothermics 29, 27–50.
Vandenberghe, D., Hossain, S.M., De Corte, F., 2003. Investigations on the origin of the equivalent dose distribution in a Dutch coversand. Radiat. Meas. 37, 433–439.
Wagner, G.A., Coyle, D.A., Duyster, J., Henjes-Kunst, F., Peterek, A., Schröder, B., Stöckhert, B., Wemmer, K., Zulauf, G., Ahrendt, H., Bischoff, R., Hejl, E., Jacobs, J., Menzel, D., Lal, N., Van den haute, P., Vercoutere, C., Welzel, B., 1997. Post-Variscan thermal and tectonic evolution of the KTB site and its surroundings. J. Geophys. Res. 102, 18221.
Wang, X.L., Wintle, A.G., Lu, Y.C., 2006. Thermally transferred luminescence in fine grained quartz from Chinese loess: basic observations. Radiat. Meas. 41, 649–658.
Warren, C.J., Singh, A.K., Roberts, N.M., Regis, D., Halton, A.M., Singh, R.B., 2014. Timing and conditions of peak metamorphism and cooling across the Zimithang Thrust, Arunachal Pradesh, India. Lithos 200, 94–110.
Whittall, K.P., MacKay, A.L., 1989. Quantitative interpretation of NMR relaxation data. J. Magn. Res. 84, 134–152.
Wintle, A.G., 2008. Fifty years of luminescence dating. Archaeometry 50, 276–312.
Wintle, A.G., Murray, A.S., 1997. The relationship between quartz thermoluminescence, photo-transferred thermoluminescence, and optically stimulated luminescence. Radiat. Meas. 27, 611–624.
Wintle, A.G., Murray, A.S., 2006. A review of quartz optically stimulated luminescence characteristics and their relevance in single-aliquot regeneration dating protocols. Radiat. Meas. 41, 369–391.
Wolfe, M.R., Stockli, D.F., 2010. Zircon (U–Th)/He thermochronometry in the KTB drill hole, Germany, and its implications for bulk He diffusion kinetics in zircon. Earth Planet. Sci. Lett. 295, 69–82.
Wright, N.J.R., 1980. Time, temperature, and organic maturation – the evolution of rank within a sedimentary pile. J. Petrol. Geol. 2, 411–425.
Wu, T.S., Kunz, A., Jaiswal, M.K., Chen, Y.G., 2012. A feasibility study on the application of luminescence dating for quartz from different rock types as a thermochronometer. Quat. Geochronol. 10, 340–344.